International Journal of Nanomedicine

Dovepress
open access to scientific and medical research

Open Access Full Text Article

ORIGINAL RESEARCH

Nanoemulsion as a strategy for improving the oral bioavailability and anti-inflammatory activity of andrographolide

This article was published in the following Dove Press journal:
International Journal of Nanomedicine

Ching-Chi Yen[1]
Yi-Chen Chen[1]
Ming-Tsang Wu[2]
Chia-Chi Wang[1,3]
Yu-Tse Wu[1,4]

[1]School of Pharmacy, College of Pharmacy, Kaohsiung Medical University, Kaohsiung, Taiwan; [2]Chinese Medicine Department, Ditmanson Medical Foundation, Chiayi Christian Hospital, Chiayi City, Taiwan; [3]PhD Program in Toxicology, College of Pharmacy, Kaohsiung Medical University, Kaohsiung, Taiwan; [4]Department of Medical Research, Kaohsiung Medical University Hospital, Kaohsiung, Taiwan

Background: Andrographolide (AG), a compound with low water solubility, possesses various pharmacological activities, particularly anti-inflammatory activity. However, its low oral bioavailability is a major obstacle to its potential use. This study developed and optimized an AG-loaded nanoemulsion (AG-NE) formulation to improve AG oral bioavailability and its protective effects against inflammatory bowel disease.

Methods: A high-pressure homogenization technique was used to prepare the AG-NE and solubility, viscosity, and droplet size tests were conducted to develop the optimized AG-NE composed of α-tocopherol, ethanol, Cremophor EL, and water. The permeability was assessed using everted rat gut sac method and in vivo absorption and anti-inflammatory effect in rats was also evaluated. The plasma concentration of AG was determined using our validated high performance liquid chromatography method, which was used to generate a linear calibration curve over the concentration range of 0.1–25 μg/mL in rat plasma (R^2>0.999).

Results: The optimized AG-NE had a droplet size of 122±11 nm confirmed using transmission electron microscopy and a viscosity of 28 centipoise (cps). It was stable at 4 and 25°C for 90 days. An ex vitro intestinal permeability study indicated that the jejunum was the optimal site for AG absorption from the optimized AG-NE, which was 8.21 and 1.40 times higher than that from an AG suspension and AG ethanol solution, respectively. The pharmacokinetic results indicate that the absorption of AG from AG-NE was significantly enhanced in comparison with that from the AG suspension, with a relative bioavailability of 594.3%. Moreover, the ulcer index and histological damage score of mice with indomethacin-induced intestinal lesions were significantly reduced by AG-NE pretreatment.

Conclusion: We conclude that the developed AG-NE not only enhanced the oral bioavailability of AG in this study but may also prove to be an effective formulation of AG for preventing gastrointestinal inflammatory disorders.

Keywords: andrographolide, nanoemulsion, intestinal permeability, oral bioavailability

Introduction

The two major forms of chronic inflammatory bowel disease (IBD) are Crohn's disease (CD) and ulcerative colitis (UC). These diseases involve chronic inflammation of the entirety or part of the digestive tract.[1] In CD, inflammation may affect the whole intestinal wall and is often transmural and discontinuous, whereas in UC, it is usually continuous, primarily affecting only the mucosal lining of the colon and rectum.[2] Worldwide, the incidence of IBD is rising. In Europe, millions of people are suffering from IBD and globally the number has reached more than 5 million individuals.[3] Although the etiology of IBD remains largely unclear, it is thought to

Correspondence: Yu-Tse Wu
School of Pharmacy, College of Pharmacy, Kaohsiung Medical University,
100, Shih-Chuan 1st Road, Kaohsiung, 80708, Taiwan
Tel +886 7 312 1101 ext 2254
Fax +886 7 312 0683
Email ytwu@kmu.edu.tw

submit your manuscript | www.dovepress.com
Dovepress
http://dx.doi.org/10.2147/IJN.S154824

be precipitated by complex interactions between oxidative stress, immunoregulation, altered inflammatory mediator levels, microbial pathogens, and genetic factors.[4] The current efficacious agents for IBD include corticosteroids,[5] anti-tumor necrosis factor (TNF) monoclonal antibodies,[6] and aminosalicylates.[7] However, these agents often result in severe and occasionally irreversible side effects such as diabetes mellitus, Cushing's syndrome, osteoporosis, and nephrotoxicity.[8] Thus, more effective and affordable treatments and a cure are urgently needed.

An increasing number of people with IBD are turning to alternative medicine, including traditional plant products.[9] Andrographolide (AG; Figure 1) is a natural diterpenoid isolated from *Andrographis paniculata*, which is a traditional remedy for fever, cold, sore throat, and various chronic infectious diseases.[10–12] Moreover, previous studies have shown that AG possesses many pharmacological activities, including anti-inflammatory,[13] antioxidative,[14] and anticancer[15] activities. A previous study showed that pretreatment with the ethanolic extract of *A. paniculata* provided significant protection against gastric ulcers.[16] Another report indicated that because of its TNF-α, interleukin (IL)-1β, and nuclear factor-κB inhibitory activities, AG has been utilized extensively for the treatment of IBD.[17,18] However, the oral bioavailability of AG is low because of its low aqueous solubility (0.07 mg/mL in water) and low oral absorption due to rapid and extensive metabolism and efflux by P-glycoprotein (P-gp) in the intestine.[19,20] Thus, to overcome the problem of low oral bioavailability, improvements to the solubility of AG and prevention of its efflux by P-gp are urgently required.

Recently, several methods have been developed to improve AG solubility and bioavailability. The hydroxypropyl-β-cyclodextrin (HP-β-CD) inclusion system was used to increase AG solubility.[20] Moreover, solid dispersion technology resulted in a five-fold increase in AG saturation solubility.[21] An optimized liquid self-microemulsifying drug delivery (SMEDD) system increased AG bioavailability 15-fold and a SMEDD pellet prepared using the extrusion–spheronization technique improved AG bioavailability approximately 13-fold.[22] Moreover, solid lipid nanoparticles inhibiting P-gp were designed to enhance AG absorption.[23] However, pharmacokinetic data for the HP-β-CD system and solid dispersion technology are lacking; thus, their effects on the absorption of AG cannot be confirmed. High surfactant concentrations in the SMEDD formulation might irritate the gastrointestinal tract, and the proposed solid lipid nanoparticle formulation lacked stability data to ensure its feasibility. In addition, the aforementioned formulations contain several materials that render the optimization of their preparation process complicated and time consuming. Thus, identifying a suitable drug delivery system for increasing the oral bioavailability of AG remains a task of great interest.

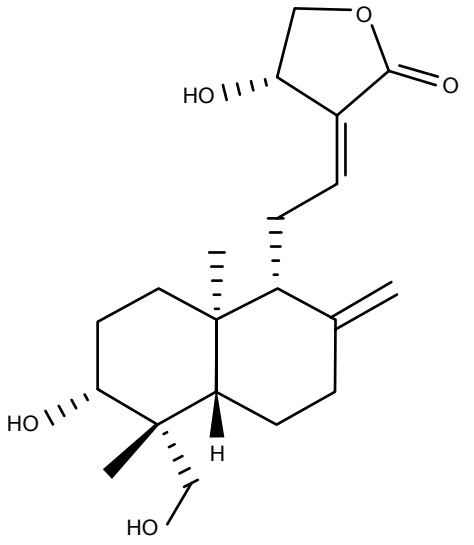

Figure 1 Chemical structure of andrographolide.

Nanoemulsion (NE) is a promising technology for enhancing the oral bioavailability of poorly soluble drugs. Oils, surfactants, and an aqueous phase are commonly used to prepare fine oil-in-water or water-in-oil NE with a droplet size usually below 200 nm.[24] In the pharmaceutical industry, NE has been extensively used as a drug delivery system to protect active ingredients against extreme conditions and maintain their effectiveness.[25,26] NE also tends to have high stability because its very small droplet size causes a large reduction in gravity force and its Brownian motion may be sufficient for overcoming gravity, and thus creaming or sedimentation can be avoided by implementing an appropriate storage period.[27] Similarly, the active components encapsulated within NE droplets can be protected from oxidation, hydrolysis, and volatilization.[28] High- and low-energy approaches constitute the two major methods for formulating NE.[29,30] In industry, the formulation of NE is performed using the high-energy approach, which utilizes mechanical devices capable of generating intense disruptive forces that break up the oil and water phases, leading to the formation of tiny oil droplets. The high-energy approach can be achieved through ultrasonicators, microfluidizers, and high-pressure homogenizers.[31–33] Among these methods, high-pressure homogenization (HPH) is a reliable method used for the fabrication of NE because it enables greater control of droplet size and a wider range of choice for composition, which in turn controls the stability, rheology, and color of the emulsion. Moreover, HPH is the most suitable

technique for industrial applications because of its ease of operation, scalability, and reproducibility.[34]

In this study, we prepared and characterized AG-loaded NE (AG-NE) by using the HPH method to enhance its aqueous solubility, intestinal penetration, and stability. We also evaluated the pharmacokinetics of AG after oral administration of optimized AG-NE to rats and compared its bioavailability with that of an AG suspension. Finally, in mice with indomethacin (INDO)-induced enteritis, the anti-inflammatory effect of the optimized AG-NE was compared with that of the AG suspension.

Materials and methods

Materials

AG (purity: ≥98.0%), sorbitan monooleate (Span® 80), polysorbate 80 (Tween® 80), polysorbate 20 (Tween® 20), dimethyl sulfoxide (DMSO), and fisetin as the internal standard (ISTD; purity: >96.0%) were obtained from Tokyo Chemical Industry (Tokyo, Japan). Polyoxyl 35 castor oil (Cremophor EL®; BASF Corporation, Ludwigshafen, Germany), α-tocopherol, tricaprylin, and INDO were supplied by Sigma-Aldrich Co. (St Louis, MO, USA). (+)-Limonene was purchased from Acros Organics (Morris, NJ, USA). Acetonitrile for high performance liquid chromatography (HPLC) and methyl tert-butyl ether (purity: ≥99.8%) were obtained from Tedia Company, Inc. (Fairfield, OH, USA).

AG solubility study

The solubility of AG in various oils (tricaprylin, triacetin, α-tocopherol, and (+)-limonene), surfactants (Span 80, Cremophor EL, Tween 80, and Tween 20), and distilled water and subsequently in oil–ethanol (1:1, v/v) mixtures was investigated by adding excess AG to these excipients, followed by vortex mixing for 30 s and shaking in a shaking water bath at 37°C for 48 h to reach equilibrium. The samples were centrifuged at 9,400× *g* for 15 min. The supernatant was collected and filtered through a 0.45-μm syringe filter. After dilution with appropriate acetonitrile, the diluted solution was injected onto a reversed-phase HPLC system for analysis of the AG concentration.

The HPLC system consisted of a LC-10AT pump, SIL-10AF autosampler, SPD-10Avp ultraviolet (UV) detector, and SCL-10Avp system controller (Shimadzu, Kyoto, Japan). Samples were separated on a reversed-phase Luna C18 column (250×4.6 mm, 5 μm; Phenomenex, Torrance, CA). The mobile phase consisted of acetonitrile and 0.01 M of Na_2HPO_4 (adjusted to pH 2.5 by using orthophosphoric acid) in the ratio of 28.6:71.4 (v/v) and was delivered at 1.0 mL/min. Prior to use, the mobile phase was filtered using a Millipore membrane filter (0.22 μm; Millipore Corporation, Bedford, MA, USA) and degassed using sonication (Branson, Danbury, CT, USA). The sample injection volume was 50 μL and the UV detection wavelength was set at 225 nm. The assay of the AG concentration was linear (R^2>0.9997) in the concentration range of 25–500 μg/mL.

AG-NE preparation

The HPH technique was used to prepare AG-NE. In brief, 30 mg of AG was dissolved in 4 g of the mixture composed of oil (α-tocopherol, triacetin, or limonene) and ethanol (1:1, w/w) as the oil phase. This mixture was mixed with 2 g of the surfactant (Tween 20 or Cremophor EL) and 6 g of water under high-speed homogenization for 10 min at 24,000 rpm (Silent crusher M Homogenizer; Heidolph Instruments GmbH & Co. KG, Schwabach, Germany). Subsequently, to fabricate stable oil-in-water AG-NE, the optimized homogenized NE was further homogenized using an HPH at 1,500 bars for 6 cycles (EmulsiFlex-C3; Avestin, Inc., Ottawa, OT, Canada).

Characterization of AG-NE

Droplet size analysis

To determine the droplet size, a 0.5-mL aliquot of AG-NE was diluted using 125 mL double-distilled water.[35] The droplet size of the AG-NE was measured at 25°C by using Photon Correlation Spectroscopy Coulter LS 230 (Beckman Coulter, Miami, FL, USA). Measurements were performed in triplicate.

Viscosity measurements

The viscosity of the AG-NE was measured using a DV2TLV viscometer (Brookfield Engineering, Middleboro, MA, USA) with a SC4-31 spindle, thermostatically controlled using a circulating water bath. All measurements were conducted at 25°C.

Transmission electron microscopy

Transmission electron microscopy (TEM) was used to determine the morphology of the optimized AG-NE. The TEM sample of the optimized AG-NE was diluted and placed on a 300-mesh copper grid coated with carbon. The sample was negatively stained using a 2% (w/v) phosphotungstic acid (PTA) solution, and excess PTA was removed. The dried grid was examined under HT7700 TEM at a voltage of 120 kV (Hitachi, Tokyo, Japan).

Stability study

The prepared AG-NE was first centrifuged at 11,180× *g* for 10 min for the observation of phase separation before

assessing the droplet size and AG content.[36] The stability study of AG-NE was performed over 90 days at 4 and 25°C by evaluating the AG content and droplet size.

Determination of drug content

Drug content was measured using the HPLC method described above. Weighted 1 mL of the AG-NE was dissolved in 10 mL acetonitrile by vortex agitation to obtain a clear supernatant and analyzed by HPLC. The encapsulation efficiency and drug loading content of AG were calculated using the following equations:

$$\text{Encapsulation efficiency (\%)} = \frac{\text{Amount of drug entrapped in AG-NE}}{\text{Initial amount of AG added}}$$

$$\text{Drug loading (\%)} = \frac{\text{Amount of drug entrapped in AG-NE}}{\text{Total amount of AG-NE}}$$

Bioanalytical method and validation

The UV detection wavelength of the HPLC system described previously was set at 225 nm. A 100 µL aliquot of rat plasma was thoroughly mixed with 20 µL of the ISTD (10 µg/mL) and then extracted with 500 µL of water-saturated methyl tert-butyl ether by vortexing for 5 min. Subsequently, the supernatant was obtained through centrifugation at 4,020× *g* and transferred to a 2-mL microtube. The extraction was repeated three times and the combined supernatant (1,300 µL) was dried in a centrifugal evaporator. Before analysis, the residue was reconstituted with 100 µL of the mobile phase.

The stock solution of AG was prepared by dissolving 50 mg of AG in 50 mL of 1 mg/mL acetonitrile. Subsequently, the stock solution was diluted with the mobile phase to prepare the working solutions at concentrations ranging from 0.5 to 125 µg/mL. The ISTD working solution (10 µg/mL) was prepared by diluting the stock fisetin solution with the mobile phase. Calibration standards were obtained by spiking 80 µL of blank rat plasma with 20 µL of AG and 20 µL of the ISTD (10 µg/mL) working solution to generate AG concentrations ranging from 0.1 to 25 µg/mL. Selectivity was confirmed by the absence of interference peaks at the retention time of AG in chromatograms of blank rat plasma. The extraction recoveries of AG were determined by comparing the peak area before and after the extraction of rat plasma standards at three quality control concentrations (0.25, 2.5, and 20 µg/mL). The limit of quantitation was determined by calculation of a signal-to-noise ratio of 10 with precision of ≤20%, and accuracy within ±20%. Intra- and inter-day variations in the results of the HPLC-UV method were assessed by analyzing three quality control concentrations in a single day and over 6 consecutive days, respectively.

Permeability evaluation

Male 7-week-old Sprague Dawley rats (body weight: 200±20 g) were purchased from the BioLASCO Experimental Animal Center (Taipei, Taiwan). The experimental protocol followed the guidelines of the Animal Protection Act and *A Guidebook for the Care and Use of Laboratory Animals* published by the government authority, and was reviewed and approved by the Institutional Animal Care and Use Committee of Kaohsiung Medical University Hospital, Kaohsiung, Taiwan (approval no. IACUC-105006). The permeability evaluation method was modified from a previous study.[37] Briefly, following anesthetization, each rat's entire small intestine was carefully isolated and flushed several times with normal saline (0.9%, w/v). The intestine was separated into three segments, namely the duodenum, jejunum, and ileum, which were immediately placed in warm Tyrode's solution. Each intestinal segment (length: approximately 4 cm) was slid onto a glass rod (diameter: 2.5 mm) and tied at one end. Subsequently, the segments were gently reverted and filled with Tyrode's solution. The open ends of the everted sacs were ligated. Subsequently, the sacs were placed in flasks containing Tyrode's solution. The AG suspension, AG ethanol solution, and AG-NE at a concentration of 50 µg/mL were separately added to the flasks. After shaking in a water bath at 37°C for 1 h, each sac was cut open. The AG content was analyzed using the developed HPLC-UV method.

Pharmacokinetic study

Male Sprague–Dawley rats were anesthetized, and polyethylene tubes were implanted into the right jugular and femoral veins for repeated sampling and intravenous injection.[38] During surgery, a heating pad was used to maintain the rats' body temperature. After surgery, all rats were allowed to recover for 1 day. According to the study design, the rats were divided into 3 groups (n=6 rats per group). In the first group, each rat was intravenously injected with the AG solution at a dosage of 5 mg/kg (AG was dissolved in normal saline and DMSO; 1:1, v/v). The second group was orally administered with the AG suspension at a dosage of 300 mg/kg (AG was suspended in 2% [w/v] carboxymethyl cellulose aqueous solution). The third group was orally administered the optimized AG-NE at a dosage of 100 mg/kg. Blood

samples were collected as blank plasma before drug administration and at predetermined time points after administration. A 250-μL blood plasma sample was manually withdrawn via a jugular vein catheter and transferred to a vial rinsed with heparin. Each sample was centrifuged at 3,000× *g* for 10 min and the plasma fraction was separated and stored at −70°C until analysis.

Anti-inflammatory activity evaluation

Male 8-week-old C57BL/6 mice (body weight: 22±2 g) were purchased from the BioLASCO Experimental Animal Center (Taipei, Taiwan). Animal experimental protocols were reviewed and approved by the Institutional Animal Care and Use Committee of Kaohsiung Medical University Hospital, Kaohsiung, Taiwan (approval no. IACUC-105039). The anti-inflammatory activity evaluation method was modified from a previous study.[39] The mice were divided into 5 groups (n=4 mice per group). Group I was the sham group. Groups II–V were injected subcutaneously with INDO at a dosage of 10 mg/kg to induce small intestinal injury and pretreated by oral administration of the drug 1 h before INDO treatment. The differences in treatment between the groups are described as follows: Group II was pretreated with a blank suspension (oral administration [PO]), Group III was pretreated with the AG suspension (300 mg/kg, PO), Group IV was pretreated with blank NE (PO), and Group V was pretreated with AG-NE (100 mg/kg, PO). Twenty-four hours after the administration of INDO, the animals were anesthetized and euthanized. The area (mm^2) of evident lesions was macroscopically measured, summed per 15 cm of the small intestine, and expressed as the ulcer index (UI). To grade the severity of gastric mucosal lesions, the UI was calculated using the following formula:

$$\begin{aligned} UI = {} & 1 \times (\text{number of lesions of grade 1}) \\ & + 2 \times (\text{number of lesions of grade 2}) \\ & + 3 \times (\text{number of lesions of grade 3}) \end{aligned}$$

Subsequently, the overall score was divided by a factor of 10.[39] Furthermore, we conducted a microscopic evaluation of small intestinal injuries. For the histological examination, two observers blinded to the treatment groups independently assessed each section by using an optical microscope and scored the section by using a previously reported histological damage scoring system.[40]

Data analysis

The results of each evaluation are expressed as mean ± standard deviation. Pharmacokinetic parameters were calculated using non-compartmental analysis.[38] SPSS v14.0 (SPSS Inc., Chicago, IL, USA) was used to conduct an analysis of variance. Differences between formulations were compared by a one-way analysis of variance followed by the least significant difference test; $p<0.05$ was considered significant.

Results and discussion

AG solubility study

The solubility values of AG in oils and surfactants are presented in Figure 2. Among all the oils, the solubility of AG in α-tocopherol (2.51±0.25 mg/mL) was the highest. Among the mixtures of oils and ethanol, the solubility values of AG in triacetin (10.57±1.05 mg/mL), α-tocopherol (10.67±2.89 mg/mL), and limonene (8.61±0.1 mg/mL) mixed with ethanol were significantly higher than that in tricaprylin (7.16±0.02 mg/mL). The solubility of the active ingredient in excipients is a crucial criterion for selecting the components of NE, and the solubility of AG in the oil phase is the most crucial criterion for screening the components. To improve the solubility of AG in the oil phase, 50% (w/w) ethanol was added to the oils. According to a previous study, mixing ethanol with oil may decrease the liquid crystalline phase, increase the microemulsion areas of the phase diagrams, and enhance the oil solubilization capacity of the microemulsions by increasing the flexibility of the surfactant film.[41] Our results showed that the oil and ethanol mixtures further significantly increased AG solubility. Thus, a mixture of oil (triacetin, α-tocopherol, or limonene) and ethanol was selected as the oil phase.

Among the surfactants, the solubility values of AG in Cremophor EL (2.57±0.19 mg/mL) and Tween 20 (3.06±0.44 mg/mL) were the highest. Both these surfactants are nonionic, used extensively because they are less toxic than ionic surfactants, and less affected by pH and ionic strength than other surfactants. Another crucial criterion is the selection of a surfactant with a suitable hydrophilic–lipophilic balance (HLB) value. An appropriate combination of surfactants with low and high HLB values leads to the formation of a stable NE upon dilution with water. To form oil-in-water NE, the HLB value must be greater than 10.[42] Finally, we selected Cremophor EL and Tween 20 with HLB values of 14 and 16.7, respectively, as the surfactants in the AG-NE formulations.

Optimization and characterization of AG-NE

The several AG-NE formulations developed in this study are listed in Table 1. Among all the formulations, F1 formed a

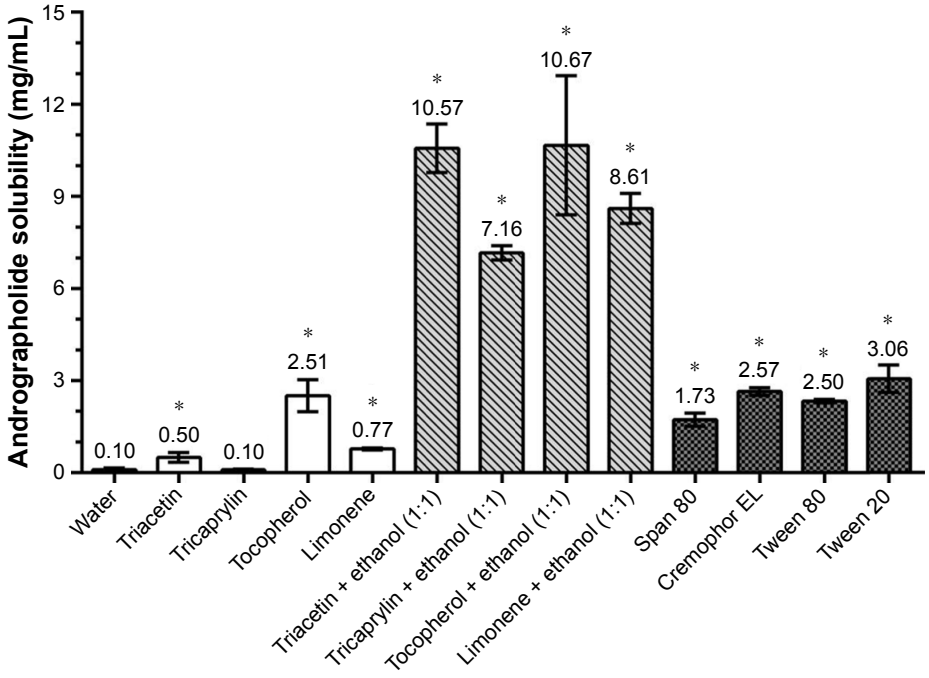

Figure 2 Solubility tests of andrographolide in different vehicles. Results were expressed as mean ± standard deviation (n=3). *Significantly different compared with the water group at $p<0.05$.

semi-solid state after high-speed homogenization for 10 min. Phase separation immediately occurred for F5. These phenomena could explain why F1 and F5 were unstable and owning larger droplet size. The droplet sizes of F3 and F4 were not within nanoscale (>1,000 nm). F2 and F6 exhibited smaller droplet sizes (122±11 and 140±53 nm, respectively), and were further tested for their stability. The results showed that the droplet size of F6 increased markedly and phase separation occurred on day 30, whereas F2 was relatively stable over the 30-day examination period. A considerable reduction in the droplet size of F2 and F6 could be attributed to the presence of the polar covalent parts in the chemical structure of Cremophor EL, namely polyethylene glycols and ethoxylated glycerol.[43] These two highly hydrophilic groups in the aqueous phase can decrease the difference in viscosity of the two immiscible phases. In addition, smaller droplets in nanoemulsions possess higher stability to gravitational separation, flocculation, and coalescence.[44] The aim of the current study was to prepare a nanoemulsion to improve AG absorption and its anti-inflammatory activity, so α-tocopherol was chosen as the oil phase due to its anti-inflammatory effect.[56] Finally, to conduct additional experiments, we selected F2 as the optimized formulation because of its nanodroplet size, low viscosity, and high stability. The size distribution and appearance of the optimized AG-NE are shown in Figure 3A.

Table 1 Composition and characterization of various AG-NE formulations

Excipients (g)	AG-NE composition					
	F1	F2	F3	F4	F5	F6
Andrographolide	0.03	0.03	0.03	0.03	0.03	0.03
α-tocopherol	2	2	–	–	–	–
Triacetin	–	–	2	2	–	–
Limonene	–	–	–	–	2	2
Ethanol	2	2	2	2	2	2
Tween 20	2	–	2	–	2	–
Cremophor EL®	–	2	–	2	–	2
Water	6	6	6	6	6	6
Droplet size (nm)	2,298±183	122±11	1,220±325	6,600±523	533±51	140±53
Viscosity (cps)	472	28	43	42	25.2	20

Notes: Droplet size expressed as mean ± standard deviation (n=3 for each formulation). The – indicates absence of the excipient.
Abbreviations: AG-NE, andrographolide-loaded nanoemulsion; cps, centipoise.

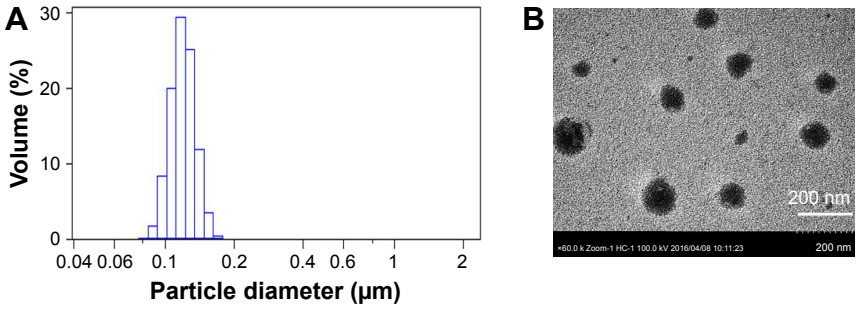

Figure 3 (**A**) Size distribution of the optimized andrographolide-loaded nanoemulsion (AG-NE) droplets determined by photon correlation spectroscopy. (**B**) Transmission electron microscopy image of the AG-NE.

Because of its ability to directly produce a high-resolution image of the formulation, TEM was used to confirm the droplet size of the optimized AG-NE. As shown in Figure 3B, the AG-NE was round with a smooth margin. Vesicles were well dispersed without aggregation and the mean size was less than 200 nm. The polydispersity index of F2 was calculated as 0.016 according to a previous study.[45] The decreases in both the particle size and the range of particle distribution can be attributed to the high-pressure homogenization procedure.[46] This small droplet size could yield favorable results for in vivo application. Furthermore, the AG-NE was stored at 4 and 25°C for 90 days and the AG content and droplet size were determined over this period. We found that the AG content remained at approximately 96% throughout the storage period (Table 2). The droplet size was not strongly affected by the storage time and no visible precipitation was observed. The encapsulation efficiency and drug loading of the optimized AG-NE were 95.7%±1.3% and 0.3%±0.004%.

Bioanalytical method validation

Figure 4 shows the representative chromatograms of blank rat plasma, blank rat plasma spiked with AG standard solution and ISTD standard solution, and a rat plasma sample obtained at 5 min after oral administration of 100 mg/kg AG-NE. The selectivity of the developed method was determined by the absence of any interference peaks during AG retention. No obvious interference peaks appeared around the retention times of the ISTD (10.5 min) or AG (16.1 min). To obtain the highest recovery of AG, the plasma was pretreated using the liquid–liquid extraction method. The extraction recoveries for AG were 105.2%±3.4%, 95.2%±3.1%, and 91.9%±5.2% for the aforementioned three quality control samples, respectively. The linear regression equation of AG in plasma was y =12,402x −11,147, and all R^2 values were greater than 0.999 within the AG concentration range of 0.1–25 μg/mL. The limit of quantification of AG was 0.1 μg/mL, and the limit of detection of AG was approximately 0.03 μg/mL. The intra-day accuracy of the results for AG in plasma was 93.8%–116.6% with a precision score of less than 6.9%. Moreover, the inter-day accuracy of the results was 85.9%–117.8% with a precision score of less than 10.3%. The high precision and accuracy indicated that the present method was reproducible and reliable for the quantitative analysis of AG in a plasma sample.

Permeability evaluation

The concentrations of AG absorbed from the AG suspension, AG ethanol solution, and optimized AG-NE through the intestinal mucosa are shown in Figure 5. The results

Table 2 AG content, AG remained, and droplet size of the optimized AG-NE (F2) stored at 4°C and 25°C over a period of 90 days

Parameters	Test period (d)					
	0	7	14	30	60	90
4°C						
AG content (mg/mL)	3.95±0.05	3.93±0.12	3.92±0.15	3.89±0.11	3.88±0.16	3.87±0.21
AG remained (%)	100.0	99.5	99.2	98.5	98.2	98.0
Droplet size (nm)	122±13	122±7	123±11	121±15	123±12	124±9
25°C						
AG content (mg/mL)	3.95±0.05	3.94±0.08	3.94±0.12	3.87±0.09	3.83±0.16	3.80±0.18
AG remained (%)	100.0	99.8	99.8	97.2	97.0	96.3
Droplet size (nm)	122±13	127±16	129±17	132±14	132±16	132±16

Note: AG content and droplet size expressed as mean ± standard deviation (n=3 for each test time).
Abbreviations: AG, andrographolide; AG-NE, andrographolide-loaded nanoemulsion; d, days.

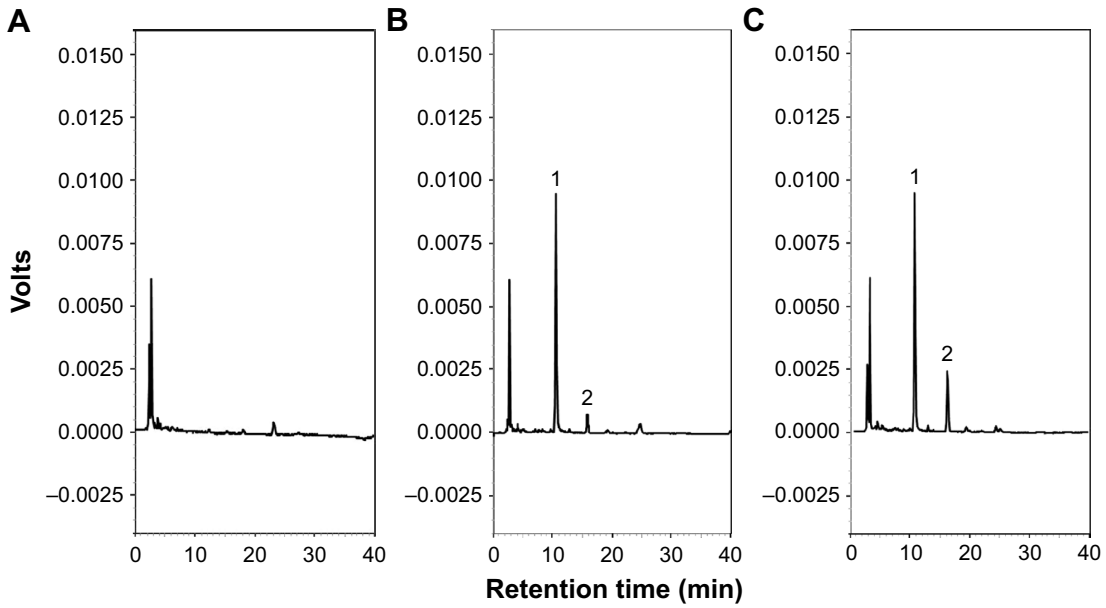

Figure 4 High-performance liquid chromatograms of (**A**) blank rat plasma, (**B**) standard andrographolide solution (0.5 μg/mL) and internal standard (ISTD) solution spiked with blank rat plasma, and (**C**) rat plasma sample at 5 min after oral administration of 100 mg/kg andrographolide-loaded nanoemulsion. Peak identification: (1): 10 μg/mL ISTD and (2): andrographolide.

indicate that the absorption of AG from the AG ethanol solution and AG-NE was enhanced in the three intestinal segments. No significant differences were observed in terms of AG absorption between the AG ethanol solution and AG-NE groups in the duodenum, whereas the intestinal permeability of AG from AG-NE was significantly increased in the jejunum and ileum compared with that from the AG ethanol solution. The jejunum was the optimal site for AG absorption from AG-NE, which was 8.21 and 1.40 times higher than those from the AG suspension and AG ethanol solution, respectively.

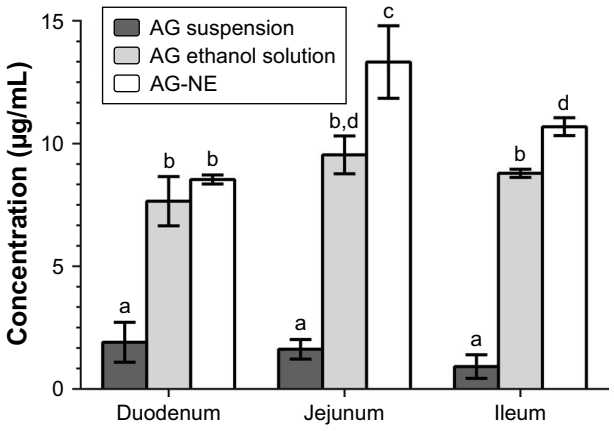

Figure 5 Concentration of andrographolide (AG) in AG suspension, AG ethanol solution, and the optimized andrographolide-loaded nanoemulsion (AG-NE) groups of different small intestine regions after incubation in AG solution (50 μg/mL) at 37°C for 1 h. Results were expressed as mean ± standard deviation (n=3). Different letters (a–d) indicate a significant difference at $p<0.05$.

The results suggest that the intestinal permeability of AG from the AG ethanol solution and optimized AG-NE was enhanced. According to a previous study, ethanol likely enhances quercetin absorption depending on the ethanol concentration because of the enhancement of quercetin solubility.[47] Although ethanol significantly enhanced the intestinal absorption of AG, the permeability of AG from AG-NE was higher than that from the AG ethanol solution in the jejunum and ileum. The precise reason is that the small droplet size of the NE enables higher adherence to the membrane during transport of the drug, thereby optimizing intestinal absorption and permeation.[48]

Pharmacokinetic study

Figure 6 illustrates the blood concentration–time profile of AG after oral administration of the optimized AG-NE and AG suspension. The areas under the curve of the AG-NE (100 mg/kg, PO) and AG suspension (300 mg/kg, PO) groups were 3.21±0.26 and 1.66±0.21 h μg/mL, respectively. The pharmacokinetic parameters are illustrated in Table 3. From the statistical analysis of the in vivo pharmacokinetic data, the relative bioavailability (%) of AG-NE to the AG suspension was 594.3%.

We have demonstrated in this study that the optimized AG-NE provided significantly enhanced bioavailability of AG compared with that provided by the AG suspension administered through the same route. The enhanced oral bioavailability can be attributed to the enhancement of AG

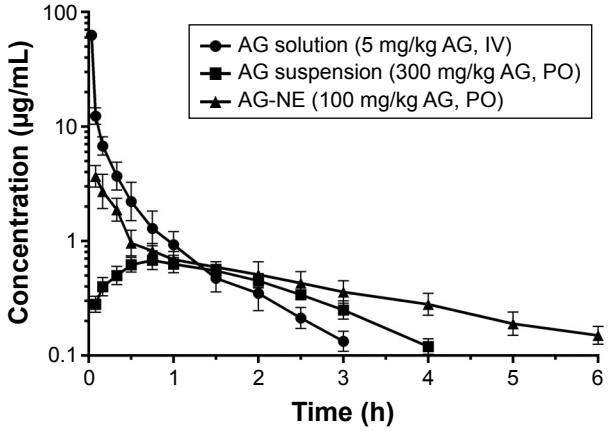

Figure 6 The plasma concentrations–time profiles of andrographolide (AG) after drug administration of AG solution (5 mg/kg, intravenous [IV] injection), AG suspension (300 mg/kg, PO), and the optimized andrographolide-loaded nanoemulsion (AG-NE) (100 mg/kg, PO) in rats. Results expressed as mean ± standard deviation (n=6).
Abbreviation: PO, oral administration.

solubility and intestinal permeability and the reduction of the droplet size in the formulation. In this study, the mean droplet size of AG-NE was approximately 122 nm and the low solubility of AG improved, as evidenced by the solubility test results. The smaller droplet size of the optimized AG-NE provided a larger surface area, consequently providing a high concentration of AG for absorption. The rat intestinal sac absorption model indicated that the permeability of AG from the AG-NE was significantly enhanced. Ye et al showed that the efflux of AG by P-gp is likely the main mechanism that decreases the permeation of AG into the ileum and colon of rat intestines and further limits the bioavailability of orally administered AG.[19] Shono et al reported that nonionic surfactants including Cremophor EL and Tween 80 may be useful pharmaceutical excipients for inhibiting the function of P-gp to increase the intestinal absorption of various drugs that can be secreted by the P-gp-mediated efflux system in the intestine.[49] Therefore, the use of Cremophor EL in the NE increases the oral exposure of AG.

Anti-inflammatory activity evaluation

We investigated the effects of AG based on those of the optimized AG-NE on the INDO-induced intestinal lesions. From Figure 7A, regarding the lesions in the small intestinal mucosa, the UI of Group II (blank suspension-treated group; 2.7±0.4) was significantly higher than that of Group I (sham group; 0.05±0.1). Figure 7B shows a similar result; the histological damage score of Group II was the highest (4.87±0.38). No significant differences were observed in terms of UI or histological damage score between Group II and Group III (AG suspension-treated group). These findings imply that INDO successfully induced intestinal inflammation in mice and the blank suspension prepared using 2% (w/w) carboxymethyl cellulose might have been pharmacologically inert. The UI and histological damage score of Group IV (blank NE-treated group) and Group V (AG-NE-treated group) were significantly lower than those of Groups II and III. No significant differences were observed in terms of UI between Groups IV and V; however, the histological damage score of Group V (2.36±0.23) was lower than that of Group IV (3.11±0.44).

Histological evaluations of small intestinal lesions under 200× microscopes are shown in Figure 8. The small intestine in Group I was histologically normal. By contrast, Figure 8B and C shows that Groups II and III exhibited marked INDO-induced intestinal ulceration and increased infiltration of inflammatory cells. However, more effective protection of the small intestinal mucosa was evidenced by a significant reduction in the width of ulceration and depth of lesions, loss of epithelial cells with less thrombus, and reduction of infiltration in the inflammatory cells in Groups IV and V, as shown in Figure 8D and E, respectively. These results suggested that pretreatment with the optimized AG-NE

Table 3 Pharmacokinetic parameters of AG after intravenous administration of AG solution and after oral administration of AG suspension and the optimized AG-NE in male rats

Parameters	AG solution (5 mg/kg, IV)	AG suspension (300 mg/kg, PO)	AG-NE (100 mg/kg, PO)
T_{max} (h)	–	0.75±0.18	0.08
C_0 or C_{max} (μg/mL)	62.68±1.09	0.73±0.08	3.78±0.88*
$t_{1/2}$ (h)	1.53±0.77	1.22±0.18	2.28±0.58*
AUC_{0-t} (h μg/mL)	9.32±1.73	1.66±0.21	3.21±0.26*
$AUC_{0-\infty}$ (h μg/mL)	10.00±1.68	1.87±0.17	3.70±0.24*
Relative bioavailability (%)	–	–	594.28±38.59

Notes: Data presented as mean ± standard deviation (n=6 for each group). *Significantly different compared between AG-NE and AG suspension groups ($p<0.05$). T_{max}, time of occurrence for maximum AG concentration; C_0/C_{max}, maximum concentration of AG; $t_{1/2}$, half-life; AUC_{0-t}, area under the plasma concentration-time curve from zero hours to time; $AUC_{0-\infty}$, area under the plasma concentration-time curve from zero hours to infinity.
Abbreviations: AG, andrographolide; AG-NE, andrographolide-loaded nanoemulsion; IV, intravenous injection; PO, oral administration.

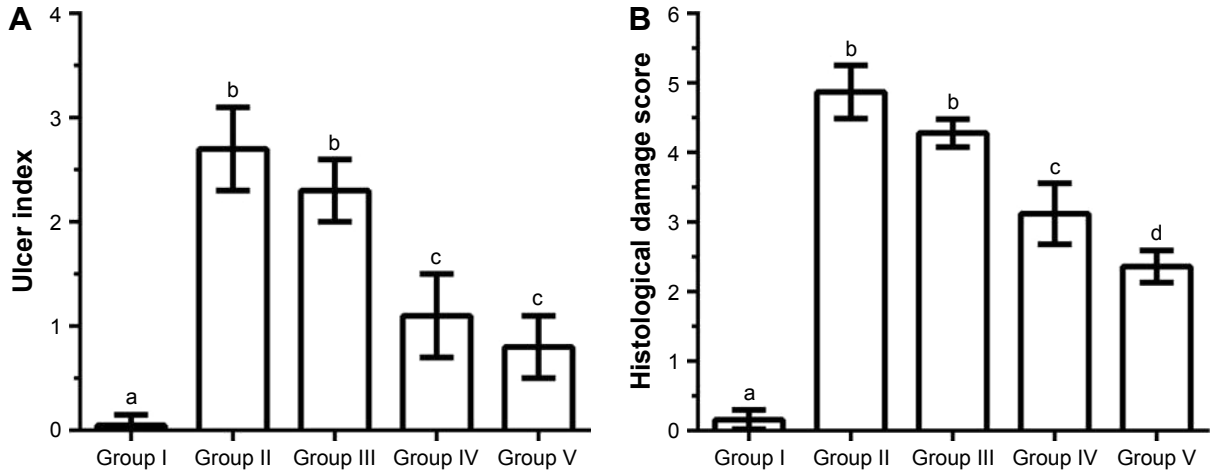

Figure 7 Effects of pre-treatment with blank suspension, andrographolide (AG) suspension, blank nanoemulsion (NE), and the optimized andrographolide-loaded nanoemulsion (AG-NE) on (**A**) ulcer index in the intestinal mucosa and (**B**) histological damage score of mice on its indomethacin-induced intestinal lesions. Group I: sham group; Others were pretreated with formulation by oral administration 1 h before treatment with indomethacin as follows: Group II was pretreated with blank suspension; group III was pretreated with AG suspension (300 mg/kg); group IV was pretreated with blank NE; and group V was pretreated with AG-NE (100 mg/kg). Results were expressed as mean ± standard deviation (n=4). Different letters (a–d) indicate a significant difference at $p<0.05$.

before INDO administration was effective for preventing and reducing inflammation of the small intestine.

Until now, several natural products such as the *Garcinia cambogia* Desr. (Clusiaceae) extract,[50] *Ginkgo biloba* L,[51] and *Zingiber officinale* Roscoe[52] have been used for the treatment of IBD. Previous studies have found that AG exhibits potent anti-inflammatory activity.[53–55] However, the therapeutic application of AG is restricted by its low solubility in water, which results in low bioavailability after oral administration. The oral bioavailability of AG was improved by the optimized AG-NE developed in this study and the anti-inflammatory potential of AG-NE was further proven. We also found that α-tocopherol present in the AG-NE partially contributed to the effects. Previous studies have shown that α-tocopherol therapy inhibits the release of proinflammatory cytokines (eg, IL-1β, IL-6, and TNF-α,) and the chemokine IL-8, and also reduces the adhesion of monocytes to the endothelium.[56] Our study results indicate that blank NE formulations containing α-tocopherol and the AG-NE can inhibit INDO-induced inflammation in the small intestine, particularly those containing the AG-NE. Moreover, AG combined with α-tocopherol in NE exerts a more effective anti-inflammatory effect than does α-tocopherol alone. Group V had a lower UI and histological damage score than did Group III. The results clearly indicate that AG-NE can increase the anti-inflammatory effect of AG.

Conclusion

In this study, we assessed the in vitro characteristics, in vivo absorption, and kinetic characteristics of an orally

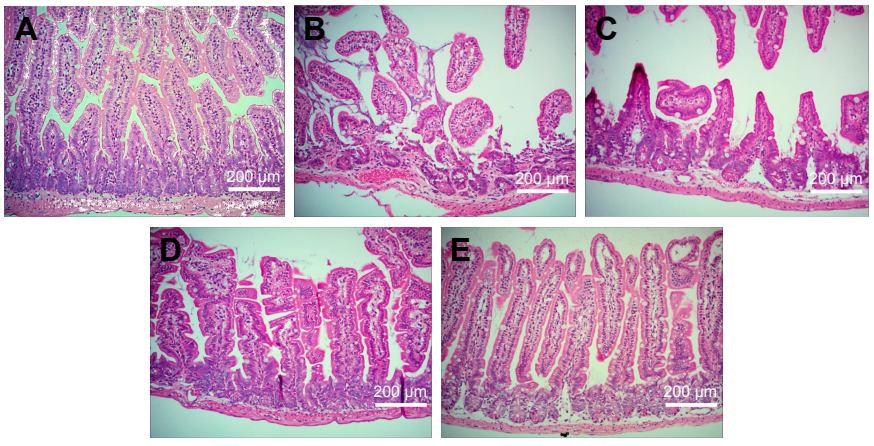

Figure 8 Representative images of small intestines. (**A**) The sham group and effect of pretreatment with (**B**) blank suspension, (**C**) andrographolide suspension, (**D**) blank nanoemulsion, and (**E**) the optimized andrographolide-loaded nanoemulsion by oral administration 1 h before treatment with indomethacin on histological appearance of indomethacin-induced small intestine lesions in mice (original magnification ×200).

administered NE containing AG and developed using HPH. The validated HPLC method was applied to study the pharmacokinetics of AG. In addition, we investigated the effect of AG-NE on INDO-induced IBD in mice. Our results indicate that AG-NE markedly enhances AG solubility and permeability. Pharmacokinetic studies show that compared with the AG suspension, the optimized AG-NE increased the relative bioavailability of AG approximately 6-fold. Furthermore, we confirmed that the AG-NE exerted a stronger anti-inflammatory effect than did the AG suspension, most likely because of increased AG absorption through the emulsion system. These results demonstrate that the AG-NE is effective for improving the oral bioavailability of AG, and thus exhibits great potential for future clinical application as an IBD treatment strategy.

Acknowledgments

Funding for this study was provided by MOST106-2113-M-037-012 from the Ministry of Science and Technology, Taiwan.

Disclosure

The authors declare no conflicts of interest in this work.

References

1. Xavier R, Podolsky D. Unravelling the pathogenesis of inflammatory bowel disease. *Nature*. 2007;448(7152):427–434.
2. Podolsky DK. Inflammatory bowel disease. *N Engl J Med*. 1991; 325(14):1008–1016.
3. Burisch J, Munkholm P. The epidemiology of inflammatory bowel disease. *Scand J Gastroenterol*. 2015;50(8):942–951.
4. Head KA, Jurenka JS. Inflammatory bowel disease part I: ulcerative colitis–pathophysiology and conventional and alternative treatment options. *Altern Med Rev*. 2003;8(3):247–283.
5. Faubion WA Jr, Loftus EV Jr, Harmsen WS, Zinsmeister AR, Sandborn WJ. The natural history of corticosteroid therapy for inflammatory bowel disease: a population-based study. *Gastroenterology*. 2001;121(2):255–260.
6. Hanauer SB, Feagan BG, Lichtenstein GR, et al. Maintenance infliximab for Crohn's disease: the ACCENT I randomised trial. *Lancet*. 2002;359(9317):1541–1549.
7. Gisbert JP, González-Lama Y, Maté J. 5-Aminosalicylates and renal function in inflammatory bowel disease: a systematic review. *Inflamm Bowel Dis*. 2007;13(5):629–638.
8. Schäcke H, Schottelius A, Döcke W-D, et al. Dissociation of transactivation from transrepression by a selective glucocorticoid receptor agonist leads to separation of therapeutic effects from side effects. *Proc Natl Acad Sci*. 2004;101(1):227–232.
9. Debnath T, Kim DH, Lim BO. Natural products as a source of anti-inflammatory agents associated with inflammatory bowel disease. *Molecules*. 2013;18(6):7253–7270.
10. Madav S, Tripathi H, Tandan, Mishra S. Analgesic, antipyretic and antiulcerogenic effects of andrographolide. *Indian J Pharm Sci*. 1995; 57(3):121–125.
11. Sinha J, Mukhopadhyay S, Das N, Basu MK. Targeting of liposomal andrographolide to *L. donovani*-infected macrophages in vivo. *Drug Deliv*. 2000;7(4):209–213.
12. Melchior J, Palm S, Wikman G. Controlled clinical study of standardized *Andrographis paniculata* extract in common cold – a pilot trial. *Phytomedicine*. 1997;3(4):315–318.
13. Shen T, Yang WS, Yi Y-S, et al. AP-1/IRF-3 targeted anti-inflammatory activity of andrographolide isolated from *Andrographis paniculata*. *Evid Based Complement Alternat Med*. 2013;2013:210736.
14. Sheeja K, Shihab P, Kuttan G. Antioxidant and anti-inflammatory activities of the plant *Andrographis paniculata* Nees. *Immunopharmacol Immunotoxicol*. 2006;28(1):129–140.
15. Wang J, Tan XF, Nguyen VS, et al. A quantitative chemical proteomics approach to profile the specific cellular targets of andrographolide, a promising anticancer agent that suppresses tumor metastasis. *Mol Cell Proteomics*. 2014;13(3):876–886.
16. Wasman S, Mahmood A, Chua LS, Alshawsh MA, Hamdan S. Antioxidant and gastroprotective activities of *Andrographis paniculata* (Hempedu Bumi) in Sprague Dawley rats. *Indian J Exp Biol*. 2011; 49(10):767–772.
17. Liu W, Guo W, Guo L, et al. Andrographolide sulfonate ameliorates experimental colitis in mice by inhibiting Th1/Th17 response. *Int Immunopharmacol*. 2014;20(2):337–345.
18. Sandborn WJ, Targan SR, Byers VS, et al. *Andrographis paniculata* extract (HMPL-004) for active ulcerative colitis. *Am J Gastroenterol*. 2013;108(1):90–98.
19. Ye L, Wang T, Tang L, et al. Poor oral bioavailability of a promising anticancer agent andrographolide is due to extensive metabolism and efflux by P-glycoprotein. *J Pharm Sci*. 2011;100(11):5007–5017.
20. Ren K, Zhang Z, Li Y, et al. Physicochemical characteristics and oral bioavailability of andrographolide complexed with hydroxypropyl-β-cyclodextrin. *Pharmazie*. 2009;64(8):515–520.
21. Bothiraja C, Shinde MB, Rajalakshmi S, Pawar AP. Evaluation of molecular pharmaceutical and in-vivo properties of spray-dried isolated andrographolide-PVP. *J Pharm Pharmacol*. 2009;61(11):1465–1472.
22. Sermkaew N, Ketjinda W, Boonme P, Phadoongsombut N, Wiwattanapatapee R. Liquid and solid self-microemulsifying drug delivery systems for improving the oral bioavailability of andrographolide from a crude extract of *Andrographis paniculata*. *Eur J Pharm Sci*. 2013;50(3):459–466.
23. Yang T, Sheng HH, Feng NP, Wei H, Wang ZT, Wang CH. Preparation of andrographolide-loaded solid lipid nanoparticles and their in vitro and in vivo evaluations: characteristics, release, absorption, transports, pharmacokinetics, and antihyperlipidemic activity. *J Pharm Sci*. 2013;102(12):4414–4425.
24. Gutiérrez J, González C, Maestro A, Sole I, Pey C, Nolla J. Nano-emulsions: new applications and optimization of their preparation. *Curr Opin Colloid Interface Sci*. 2008;13(4):245–251.
25. Madene A, Jacquot M, Scher J, Desobry S. Flavour encapsulation and controlled release – a review. *Int J Food Sci Technol*. 2006;41(1):1–21.
26. Vyas TK, Shahiwala A, Amiji MM. Improved oral bioavailability and brain transport of Saquinavir upon administration in novel nanoemulsion formulations. *Int J Pharm*. 2008;347(1):93–101.
27. Lovelyn C, Attama AA. Current state of nanoemulsions in drug delivery. *J Biomater Nanobiotechnol*. 2011;2(5A):626–639.
28. Kotta S, Khan AW, Pramod K, Ansari SH, Sharma RK, Ali J. Exploring oral nanoemulsions for bioavailability enhancement of poorly water-soluble drugs. *Expert Opin Drug Deliv*. 2012;9(5):585–598.
29. Vandamme TF, Anton N. Low-energy nanoemulsification to design veterinary controlled drug delivery devices. *Int J Nanomedicine*. 2010; 5:867–873.
30. Wang X, Jiang Y, Wang Y-W, Huang M-T, Ho C-T, Huang Q. Enhancing anti-inflammation activity of curcumin through O/W nanoemulsions. *Food Chem*. 2008;108(2):419–424.
31. Leong T, Wooster T, Kentish S, Ashokkumar M. Minimising oil droplet size using ultrasonic emulsification. *Ultrason Sonochem*. 2009; 16(6):721–727.
32. Qian C, McClements DJ. Formation of nanoemulsions stabilized by model food-grade emulsifiers using high-pressure homogenization: factors affecting particle size. *Food Hydrocoll*. 2011;25(5): 1000–1008.

33. Jafari SM, He Y, Bhandari B. Optimization of nano-emulsions production by microfluidization. *Eur Food Res Technol*. 2007;225(5–6):733–741.
34. Schultz S, Wagner G, Urban K, Ulrich J. High-pressure homogenization as a process for emulsion formation. *Chem Eng Technol*. 2004;27(4):361–368.
35. Bouchemal K, Briancon S, Perrier E, Fessi H. Nano-emulsion formulation using spontaneous emulsification: solvent, oil and surfactant optimization. *Int J Pharm*. 2004(1–2);208:241–251.
36. Fofaria NM, Qhattal HSS, Liu X, Srivastava SK. Nanoemulsion formulations for anti-cancer agent piplartine – Characterization, toxicological, pharmacokinetics and efficacy studies. *Int J Pharm*. 2016;498(1–2):12–22.
37. Tsai Y-M, Chang-Liao W-L, Chien C-F, Lin L-C, Tsai T-H. Effects of polymer molecular weight on relative oral bioavailability of curcumin. *Int J Nanomedicine*. 2012;7:2957–2966.
38. Chang C-W, Wang C-Y, Wu Y-T, Hsu M-C. Enhanced solubility, dissolution, and absorption of lycopene by a solid dispersion technique: the dripping pill delivery system. *Powder Technol*. 2016;301:641–648.
39. Yoriki H, Naito Y, Takagi T, et al. Hemin ameliorates indomethacin-induced small intestinal injury in mice through the induction of heme oxygenase-1. *J Gastroenterol Hepatol*. 2013;28(4):632–638.
40. Imaoka H, Ishihara S, Kazumori H, et al. Exacerbation of indomethacin-induced small intestinal injuries in Reg I-knockout mice. *Am J Physiol Gastrointest Liver Physiol*. 2010;299(2):G311–G319.
41. Garti N, Yaghmur A, Leser ME, Clement V, Watzke HJ. Improved oil solubilization in oil/water food grade microemulsions in the presence of polyols and ethanol. *J Agric Food Chem*. 2001;49(5):2552–2562.
42. Kommuru TR, Gurley BA, Khan M, Reddy IK. Self-emulsifying drug delivery systems (SEDDS) of coenzyme Q 10: formulation development and bioavailability assessment. *Int J Pharm*. 2001;212(2):233–246.
43. Tang SY, Manickam S, Wei TK, Nashiru B. Formulation development and optimization of a novel Cremophore EL-based nanoemulsion using ultrasound cavitation. *Ultrason Sonochem*. 2012;19(2):330–345.
44. Tadros T, Izquierdo P, Esquena J, Solans C. Formation and stability of nano-emulsions. *Adv Colloid Interface Sci*. 2004;108–109:303–318.
45. Clemente Z, Castro VLSS, Moura MAM, Jonsson CM, Fraceto LF. Toxicity assessment of TiO_2 nanoparticles in zebrafish embryos under different exposure conditions. *Aquat Toxicol*. 2014;147:129–139.
46. Floury J, Desrumaux A, Lardières J. Effect of high-pressure homogenization on droplet size distributions and rheological properties of model oil-in-water emulsions. *Innov Food Sci Emerg Technol*. 2000;1(2):127–134.
47. Azuma K, Ippoushi K, Ito H, Higashio H, Terao J. Combination of lipids and emulsifiers enhances the absorption of orally administered quercetin in rats. *J Agric Food Chem*. 2002;50(6):1706–1712.
48. Monteiro LM, Lione VF, do Carmo FA, et al. Development and characterization of a new oral dapsone nanoemulsion system: permeability and in silico bioavailability studies. *Int J Nanomedicine*. 2012;7:5175–5182.
49. Shono Y, Nishihara H, Matsuda Y, et al. Modulation of intestinal P-glycoprotein function by cremophor EL and other surfactants by an in vitro diffusion chamber method using the isolated rat intestinal membranes. *J Pharm Sci*. 2004;93(4):877–885.
50. dos Reis SB, de Oliveira CC, Acedo SC, et al. Attenuation of colitis injury in rats using *Garcinia cambogia* extract. *Phytother Res*. 2009;23(3):324–329.
51. Kotakadi VS, Jin Y, Hofseth AB, et al. *Ginkgo biloba* extract EGb 761 has anti-inflammatory properties and ameliorates colitis in mice by driving effector T cell apoptosis. *Carcinogenesis*. 2008;29(9):1799–1806.
52. El-Abhar HS, Hammad LN, Gawad HSA. Modulating effect of ginger extract on rats with ulcerative colitis. *J Ethnopharmacol*. 2008;118(3):367–372.
53. Lee K-C, Chang H-H, Chung Y-H, Lee T-Y. Andrographolide acts as an anti-inflammatory agent in LPS-stimulated RAW264.7 macrophages by inhibiting STAT3-mediated suppression of the NF-κB pathway. *J Ethnopharmacol*. 2011;135(3):678–684.
54. Abu-Ghefreh AA, Canatan H, Ezeamuzie CI. In vitro and in vivo anti-inflammatory effects of andrographolide. *Int Immunopharmacol*. 2009;9(3):313–318.
55. Xia Y-F, Ye B-Q, Li Y-D, et al. Andrographolide attenuates inflammation by inhibition of NF-κB activation through covalent modification of reduced cysteine 62 of p50. *J Immunol*. 2004;173(6):4207–4217.
56. Singh U, Jialal I. Anti-inflammatory effects of α-tocopherol. *Ann N Y Acad Sci*. 2004;1031(1):195–203.